



Trade Science Inc.

ISSN : 0974 - 7486

Volume 8 Issue 8

# Materials Science

An Indian Journal

Full Paper

MSAIJ, 8(8), 2012 [303-308]

## Microstructural and hardness of spray deposited Al-30Mg<sub>2</sub>Si-2Cu alloy in solutionized and aged conditions

Dayanand M.Goudar<sup>1\*</sup>, G.B.Rudrakshi<sup>2</sup>, G.Jagannatha Reddy<sup>3</sup>, V.C.Srivastava<sup>4</sup>, Jagdish Vagmode<sup>5</sup>

<sup>1</sup>Department of Mechanical Engineering, Tontadarya College of Engineering, Gadag-582101, (INDIA)

<sup>2</sup>Department of Mechanical Engineering, Basveshwar Engineering College, Bagalkot-58710, (INDIA)

<sup>3</sup>Department of Mechanical Engineering, Rao Bahadur Y.Mahabaleswarappa Engineering College, Bellary-583104, (INDIA)

<sup>4</sup>Research and Development Center, Jindal Steel Works, Bellary-583275, (INDIA)

<sup>5</sup>Metal Extraction and Forming Division, National Metallurgical Laboratory, Jamshedpur-831007, (INDIA)

E-mail: dayanand\_goudar@yahoo.co.in; rudrakshi\_gb@rediffmail.com; jagsha1964@yahoo.com;

vcsrivas@nmlindia.org; jagadeesh.vagmode@jsw.in

Received: 6<sup>th</sup> February, 2012 ; Accepted: 6<sup>th</sup> March, 2012

### ABSTRACT

An Al-30Mg<sub>2</sub>Si- 2Cu alloy was produced by spray casting and the secondary processing such as hot compression and heat treatment were carried out. The coarsening behavior, distribution and size of the Mg<sub>2</sub>Si precipitates, the influence of subsequent heat treatment on the microstructure were investigated. Uniform distribution of Mg<sub>2</sub>Si was achieved by spray casting. The hardness tests were conducted on spray deposited, secondary processed and heat treated alloys. The results indicate that spray casting has strong influence on microstructure and hardness of the material. The microstructural refinement of the alloy was enhanced during hot compression. The alloying with copper lead to further increase in strength by age hardening due to precipitation Al<sub>2</sub>Cu phase. A significant improvement in hardness was observed after hot compression and heat treatment.

© 2012 Trade Science Inc. - INDIA

### KEYWORDS

Al-Mg<sub>2</sub>Si alloy;  
Spray deposition;  
Microstructure;  
Age hardening;  
Hardness.

### INTRODUCTION

High strength and light weight aluminum alloys are the demand of present day automobile industry. Alloying Al with high contents of Mg and Si (>15 wt % Mg<sub>2</sub>Si) gives an increased stiffness as well as significant reduction in density. However, the required fine distribution of the Mg<sub>2</sub>Si particles in the aluminum matrix is difficult by conventional casting methods, due to excessive slag formation, high porosity, high solubility of hydrogen in

such melts<sup>[1-3]</sup> and low solidification rate<sup>[4]</sup>. Spray casting offers the possibility of producing these alloys with very fine and homogeneous microstructures<sup>[4]</sup> due to high solidification rates achieved. Post processing such as hot compression /extrusion and heat treatment are generally carried out to optimize mechanical properties. Besides, the formation of undesired phase morphologies is suppressed by this technique<sup>[5,6]</sup>. Therefore, in the present study, Al-30Mg<sub>2</sub>Si-2Cu alloy was spray formed and characterized in terms of microstruc-

## Full Paper

tural features and mechanical properties in the spray formed as well as in different heat treated conditions.

### EXPERIMENTAL PROCEDURE

The chemical composition of the alloy, used in this work, was 17.8%Si, 10.4%Al, 1.8%Cu, 0.5%Fe, 0.2%Ni and 0.6%Zn. The details of the spray forming setup used are described elsewhere<sup>[7]</sup>. The alloy was atomized with nitrogen gas and deposited onto a copper substrate, consolidated to form a coherent preform of as shown in Figure 1. The parameters of spray deposition processing (SDP) are systematically represented in TABLE 1. The preform was cut into rectangular billets and hot pressed at a temperature of 480°C after soaking for 60min. The density measurements were carried out by means of Archimedes method. Solution heat treatment was carried out in a muffle furnace at 530°C for 2 h followed by water quenching. Artificial aging was performed at a temperature of 180°C and holding the specimens for different time's viz. 1 h, 2 h, 4 h, 6 h and 12 h. The specimens were prepared from sprayed deposit, hot compressed as well as aged samples to study their microstructural features and compositions of constituent phases using optical microscope, scanning electron microscope and energy dispersive X-ray spectroscopy (EDS). The hardness of the specimens was



Figure 1 : Spray deposited preform

TABLE 1 : Primary process parameters

Process parameters	Value
Melt superheat (°C)	100
Melt flow (kg/min)	2
Gas-to-metal ratio (G/M)	1.82
Substrate distance from nozzle (mm)	390

investigated using micro-hardness tester (Mitutoyo ATK-600 hardness.) at a load of 300gms.

### RESULTS AND DISCUSSION

#### Microstructure

A coarse microstructure of primary  $\beta$ -Mg<sub>2</sub>Si phase was formed as evidenced in optical micrograph of the as-cast alloy, as shown in Figure 2. This is due to large solidification range (interval between liquidus and solidus) for higher Mg<sub>2</sub>Si content in the pseudo binary section and slow cooling rate<sup>[8]</sup>. The SEM image of as-cast alloy (Figure 3a) shows the existence of primary Mg<sub>2</sub>Si ( $\beta$ ) phase in the form of coarse platelet and polygonal blocks with clear sharp corners having uneven distribution in the  $\alpha$ -Al matrix. The sharp edges of these

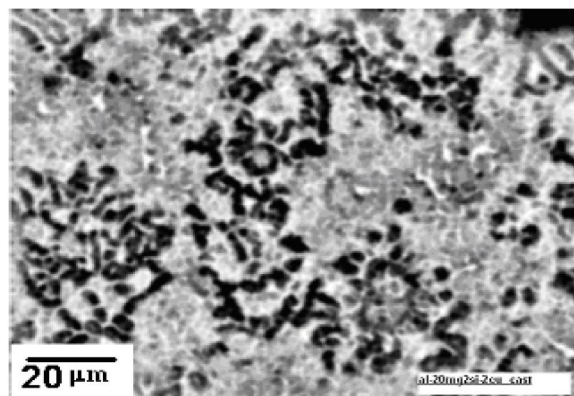


Figure 2 : Optical microstructure of as-cast alloy

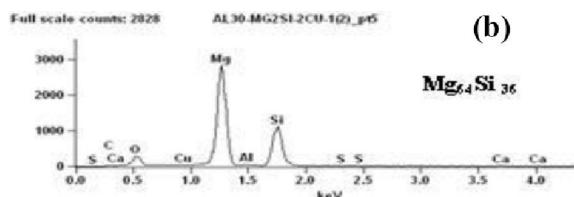
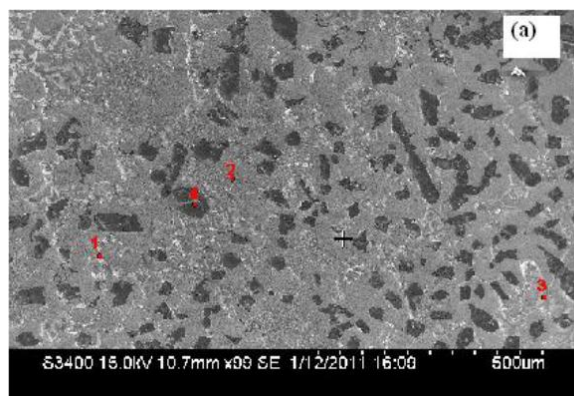


Figure 3 : (a) SEM micrograph of as-cast alloy (b) EDS spectrum of large gray Mg<sub>2</sub>Si particles

large faceted intermetallic particles and Al matrix lead to stress concentration and final failure. Fine fiber-like phase was observed as a fine bright eutectic structure (Point 1, Figure 3) with acicular, clavicorn or vermicorn having eutectic phases of  $\text{Al}_{26}\text{Mg}_{46}\text{Si}_{27}$  (Point 4, Figure 3b)  $\text{Al}_2\text{Cu}$  ( $\theta$ ), and Q ( $\text{Al}_{82}\text{Cu}_5\text{Mg}_5\text{Si}_7$ ). The exact composition of Q phase is unknown but it is usually stated as  $\text{Al}_{15}\text{Cu}_2\text{Mg}_8\text{Si}_6$  or  $\text{Al}_4\text{CuMg}_5\text{Si}_4$  or  $\text{Al}_4\text{Cu}_2\text{Mg}_8\text{Si}_7$  or  $\text{Al}_3\text{Cu}_2\text{Mg}_9\text{Si}_7$ . The composition of each phase is represented in the TABLE 2.

TABLE 2 : EDS analysis of as-cast alloy

Location	Composition (mass %)			
	Al	Mg	Si	Cu
PT1	68.01	3.65	6.47	11.54
PT2	94.48	0.20	0.59	1.60
PT3	22.60	36.17	24.76	Nil
PT4	0.69	49.91	32.21	Nil

Optical micrograph of spray deposited alloy is shown in Figure 4. The microstructure indicates uniform distribution of primary  $\text{Mg}_2\text{Si}$  ( $\beta$ ) phase particles with globular shape (some of them still possess an irregular shape) in the supersaturated  $\alpha$ -Al matrix. It is observed that the average size of these particles reduced to less than  $7\ \mu\text{m}$  as against  $60\text{--}70\ \mu\text{m}$  in as cast condition. The nucleation and growth rate were influenced by cooling rate. As the cooling rate increased during atomisation, the nucleation rate of  $\beta$  phase increased and growth rate was suppressed due to high undercooling. Thus, large amount of fine and uniformly distributed  $\beta$  phase was formed. Because of the high content of magnesium and silicon, agglomeration of particles can be observed. During deposition, small particle which were agglomerate together were assumed to be one large particle. The initial size of  $\text{Mg}_2\text{Si}$  ( $\beta$ ) depends significantly on the spray deposition conditions. The formation of pores of various sizes (Figure 4) in the spray deposit was 14%. The main causes of the porosity formation could be the gas entrapped between arriving droplets and pre-existing in the deposit, another possibility could be the evolution of hydrogen from the feed stock. The amount and appearance of porosity in spray deposits is strongly governed by and is a complex interplay of process parameters like melt superheat, G/M ratio and deposition distance. The porosity can be minimized by judicious selection of these factors. The SEM/EDX of spray deposited alloy

showed  $\text{Al}_{82}\text{Cu}_5\text{Mg}_5\text{Si}_7$  (Q),  $\text{Mg}_{64}\text{Si}_{36}$  ( $\beta$ ),  $\text{Al}_{54}\text{Mg}_9\text{Si}_{13}\text{Cu}_{23}$ ,  $\text{Al}_{84}\text{Cu}_{17}$  ( $\theta$ ) and  $\text{Al}_{26}\text{Mg}_{46}\text{Si}_{27}$  Phases ( $\beta$ ) which are shown in Figure 5a and figure 5b. The EDS for different phases in spray-deposited alloy is shown in the TABLE 3. The primary fine  $\text{Mg}_2\text{Si}$  ( $\beta$ ) particles are interconnected dispersoids distributed in  $\alpha$ -Al matrix and intermetallic phases ( $\theta$  and Q) with platelet irregular shape with sharp edges having different aspect ratios were observed. It is possible to recognize an equiaxed appearance of  $\alpha$ -Al phase is remarkable feature in the observed microstructure and is ascribed to the extensive fragmentation and coarsening

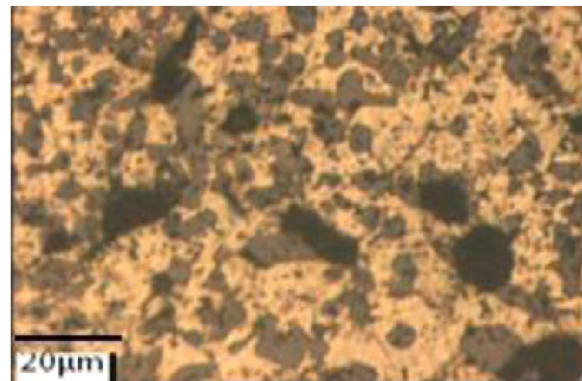


Figure 4 : Optical microstructure of sprayed alloy

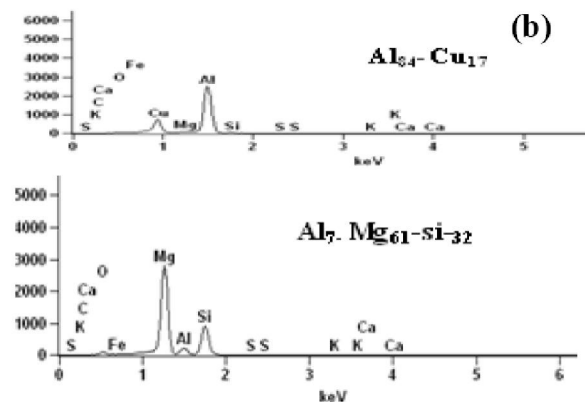
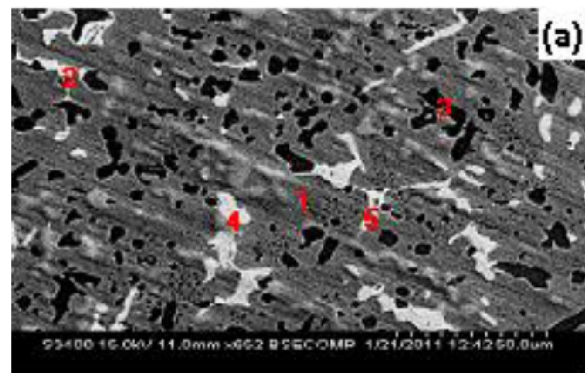


Figure 5 : (a) SEM micrograph of spray deposited alloy; (b) EDS spectrum of  $\theta$  and Q phases

## Full Paper

TABLE 3 : EDS analysis of spray deposited alloy

Location	Composition (mass %)			
	Al	Mg	Si	Cu
PT1	96.07	1.36	0.72	18.97
PT2	25.58	27.98	26.77	Nil
PT3	6.93	53.88	33.21	Nil
PT4	45.27	15.35	27.49	Nil
PT5	67.02	0.99	0.61	30.80

of solid phases during the buildup of the deposit.

Figure 6 shows the backscattered image of the sample hot pressed at 480°C. The microstructure shows reduction in porosity, partial recrystallization and the secondary phases ( $\theta$  and Q) are fragmented to fine particles. There was no significant change in size and morphology of high content of hard coarse Mg<sub>2</sub>Si ( $\beta$ ) particles. When the alloy is stressed, the deformation in material is evenly distributed and consequently the resistance of alloy to stress concentration is improved, resulting in a material with enhanced mechanical properties.

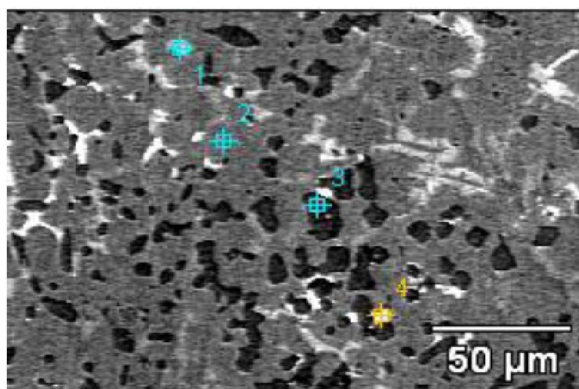


Figure 6 : SEM photograph of hot pressed spray deposited alloy

### Microstructure of alloy after heat treatment

Figures 7 and 8 show optical and SEM images of hot pressed and solution treated alloy, respectively. The EDS for different phases in spray-deposited, hot pressed and solution treated sample is shown in the TABLE 4. Magnesium and copper rich phases which have been formed during solidification are dissolved into  $\alpha$ -Al matrix during solution treatment. Fragmentation, spheroidisation and coarsening occurred for  $\beta$ -Mg<sub>2</sub>Si phase and Q (Al<sub>49</sub>-Mg<sub>19</sub>-si<sub>27</sub>-Cu<sub>8</sub>) phase. Rapid cooling freezes the new created structure and large amount of Q phase precipitates were formed around the Mg<sub>2</sub>Si phase interface (Point 2, Figure 8a). Easier and faster diffusion occurs along the

grain boundaries and interfaces, obviously the Mg<sub>2</sub>Si : Al interface play significant role during the morphological change of Mg<sub>2</sub>Si particles. If the quenching rate is sufficiently high, solute is retained in solid solution and large numbers of vacancies remain without any change. On the other hand if the quenching rate is low, particles precipitate heterogeneously at grain boundaries or defects resulting in a reduction in super saturation of solute and

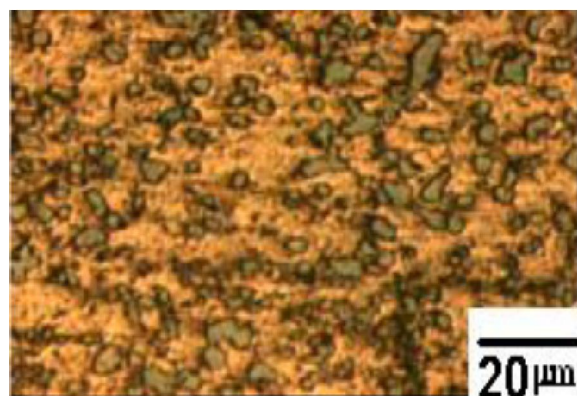


Figure 7 : Microstructures of solution heat treated spray deposited and hot pressed alloy

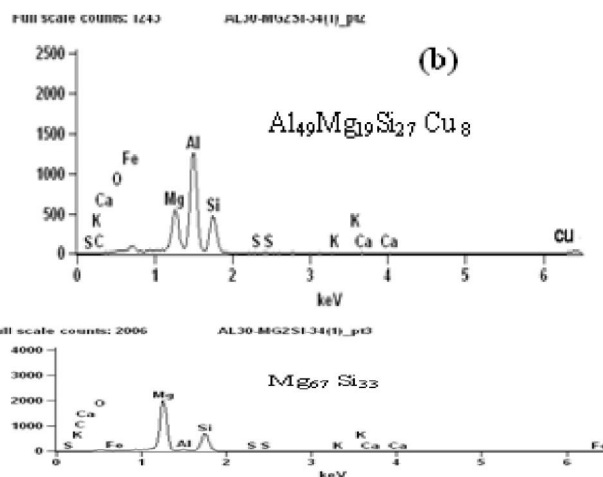
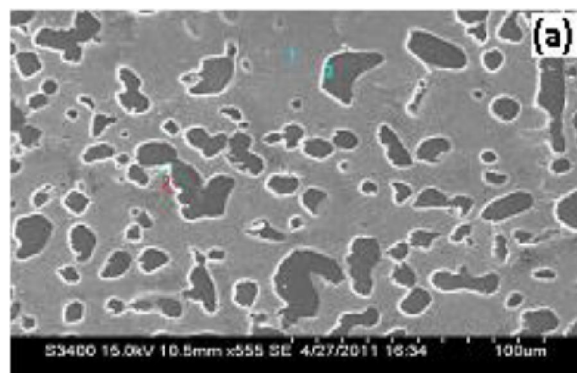


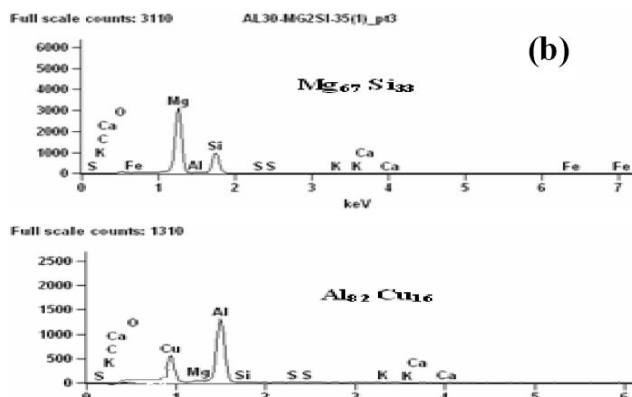
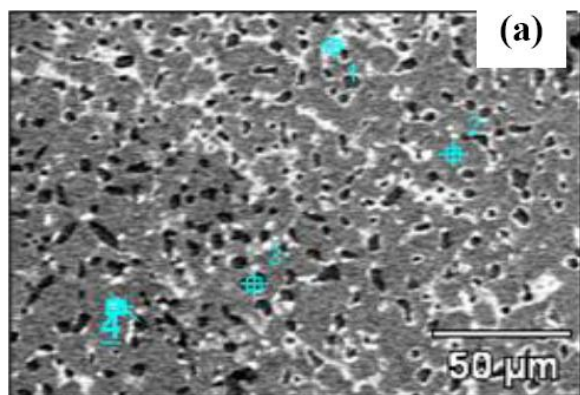
Figure 8 : (a) SEM micrograph of solution heat treated spray deposited and hot pressed alloy (b) EDS spectrum of  $\beta$ -Mg<sub>2</sub>Si and Q (Al<sub>49</sub>-Mg<sub>19</sub>-si<sub>27</sub>-Cu<sub>8</sub>) phase.

**TABLE 4 : EDS analysis of spray deposited, hot compressed solution heat treated alloy**

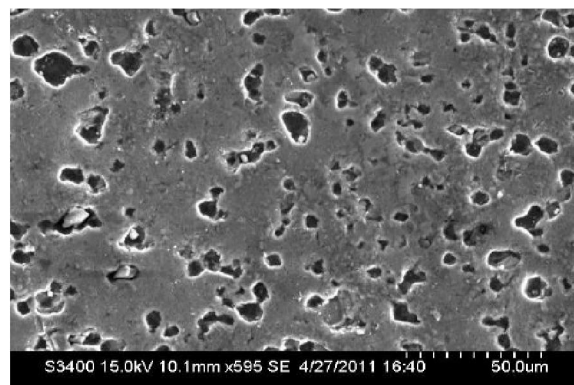
Location	Composition (mass %)			
	Al	Mg	Si	Cu
PT1	76.61	0.70	0.46	20.00
PT2	46.18	15.87	26.38	10.50
PT3	2.13	55.95	35.26	Nil

thereby a lower maximum strength after aging. The formation of induced residual stresses in the casting is the main drawback associated with the quick cooling.

The artificial ageing treatment is designed to produce optimum size, distribution, constitution and morphology of precipitates and amount of solute in solid solution. Controlled ageing of solution treated alloys engenders high hardness, with a decrease of ductility<sup>[9]</sup>. Figure 9a shows the SEM image of sample aged at 180°C for 2 hours. TABLE 5 shows the EDS data for different phases in age hardened alloy. The increase of Al-Mg<sub>2</sub>Si eutectic phase and area fraction of precipitation along the interface of primary Mg<sub>2</sub>Si ( $\beta$ ) phase could be easily observed. The  $\beta$  phase re-precipitates in a very fine form during aging. Precipitation of  $\theta$ -Al<sub>2</sub>Cu phase leads to increase in hardness and a peak is observed in

**Figure 9 : (a) SEM micrograph of age hardened alloy (ageing time 2 h); (b) EDS spectrum of  $\beta$  and  $\theta$  phases****TABLE 5 : EDS analysis artificial age hardened alloy**

	Mg	Al	Si
PT1	15.83	47.55	25.47
PT2	0.39	97.31	0.18
PT3	60.54	0.61	34.45
PT4	0.99	67.02	0.61

**Figure 10 : SEM photograph of age hardened alloy (1 h)**

the ageing curve<sup>[10]</sup>. It observed that fine and uniform distribution of Al<sub>82</sub>Cu<sub>16</sub> ( $\theta$ ) phase and Al<sub>51</sub>Mg<sub>19</sub>Si<sub>26</sub>Cu<sub>4.3</sub> (Q) phase in and  $\alpha$ -Al matrix is present in figure 10. There is also an increase in Mg<sub>67</sub>Si<sub>33</sub> ( $\beta$ ) (Point 3, Figure 9a) phase area fraction. These fine  $\beta$  precipitates combined with the  $\theta$  precipitates can significantly increase the strength of the alloy. Upon additional aging the particles grow with an increase in coherency strain until interfacial bond strength is exceeded and they become incoherent. After aging the alloys for 1 h and 2 h, SEM images were obtained and are presented in Figure 9 and 10. Precipitates in the alloy kept for 2 h is more compared to the one which is aged for 1h.

## EFFECT OF HEAT TREATMENT ON HARDNESS

Figure 11 shows the VHN hardness of the as cast, sprayed deposited, hot pressed and heat treated alloys and was measured by applying a load of 300g. The hardness of spray deposited alloy is higher than the as cast, which may be attributed to a large amount of fine and uniformly distributed of Mg<sub>2</sub>Si ( $\beta$ ) and Al<sub>2</sub>Cu( $\theta$ ) phase in  $\alpha$ -Al matrix. The  $\beta$  phase provides an appreciable impediment to plastic deformation. The fragmented intermetallics, fine and uniformly distributed precipitates as well as reduction in porosity leads to high hardness. The hardness of hot pressed alloy is higher

## Full Paper

than the as cast and as deposited alloy. The deformation caused by the indentation was restricted by the fine refined intermetallics phases ( $\theta$  and Q). The hardness of solution treated alloy was 121 HV, due to rapid cooling from the solutionizing temperature. Point defects and line defects are formed around the Mg<sub>2</sub>Si particles due to large thermal stress generated by the significant difference of thermal expansion coefficients between Mg<sub>2</sub>Si and Al. These defects interact with the dislocations and caused the increase of the hardness, and the degree of supersaturation of solute atoms was higher in solution heat treated alloy which led to increase in the hardness. The hardness of aged alloy is higher than the solution treated alloy. During ageing, as precipitation proceeds, the size and number of precipitates increases and leads to appreciable impediment to plastic deformation. The alloy reaches the peak hardness of 174 HV at 2h of aging time. As the aging time increased hardness decreased because precipitates transformed gradually from metastable state to the stable state, and finally to an incoherent interface between precipitates

and matrix. The second peak is due to the occurrence of the lattice strain, which the dislocations must be forced through causing the maximum hardness. Gradually, the hardness decreases, beyond second peak, due to the release of lattice strain and growth of precipitates

## CONCLUSIONS

1. The microstructure of spray deposited Al-30Mg<sub>2</sub>Si-2Cu alloy has finer and equiaxed particles, refined  $\alpha$ -Al matrix and near uniform distribution of Mg<sub>2</sub>Si particles in  $\alpha$  Al matrix. Hot compressed spray deposits lead to a significant reduction of porosity level of the alloy. After solution heat treatment an important reduction and spheroidisation of the Mg<sub>2</sub>Si particles occurs.
2. The increased hardness of the deposit against as-cast alloy increased by 25%. The peak hardness level during ageing was reached after about 2 h. The peak hardness of heat treated alloy is higher than as cast and deposited alloys and is approximately 97% and 58%, respectively.

TABLE 6 : Sample nomenclature of alloy

S.No.	Alloy	Sample nomenclature
1	As cast alloy	A
2	Sprayed alloy	B
3	Sprayed & hot compressed alloy	C
4	Soln heat treated at 530c -2hr	D
5	Age hardened - 0.5 hour	E
6	Age hardened - 1 hour	F
7	Age hardened - 2 hour	G
8	Age hardened - 4 hour	H
9	Age hardened - 8 hour	I
10	Age hardened - 12 hour	J

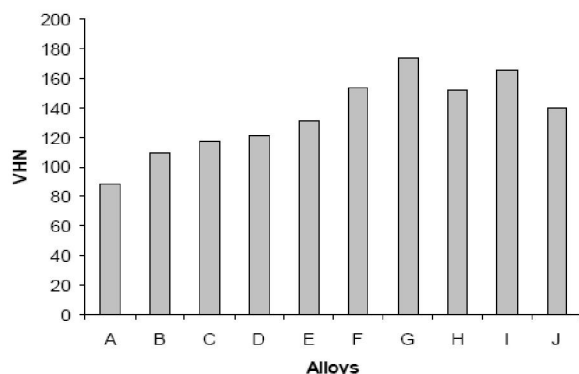


Figure 11 : Hardness values of the alloys before and after ageing

## REFERENCES

- [1] Frommeyer, G.Beer, S.Von Oldernberg; K.Zeitschrift fur Metallkunde. **85**, 372-377 (1994).
- [2] J.Zhang, Z.Fan, Y.-Q.Wang, B.-L.Zhou; Materials Science and Technology, 913-918 (2000).
- [3] U.Bischofberger; Deutsches Paten –und Markenamt, No. DE102004-007704.5, (2004).
- [4] K.Hummert, Frech, M.Schwagereit; Metall, **9**, 496-500 (1999).
- [5] N.Ellendt, V.Uhlenwinkel, O.Stelling, A.Irretier, O.Kessler; Materials Science Forum, 437-440 (2007).
- [6] A.K.Srivastav, R.C.Aananndani, A.Dhar, A.K.Gupta; Mater.Sci.Eng., **A9(587)**, 304-306 (2001).
- [7] G.B.Rudrakshi, V.C.Srivastava, J.P.Pathak, S.N.Ojha; Mater.Sci.Eng., **A383**, 30-38 (2004).
- [8] P.Krug; Konstruktion, IW6-IW7 (2008).
- [9] O.Stelling, N.Ellendt, V.Uhlenwinkel, A.von Hehl, H.W.Zoch; International Heat Treatment and Surface Engineering, **4(1)**, 41-46 (2010).
- [10] Q.D.Qin, Y.G.Zhao, C.Liu, P.J.Cong, W.Zhou, Y.H.Liang; Journal of Alloys and Compounds, **416**, 143-147 (2006).